Biochemistry and Biophysics Reports 32 (2022) 101345

Contents lists available at ScienceDirect

Biochemistry and Biophysics Reports

journal homepage: www.elsevier.com/locate/bbrep

Oxidized low-density lipoprotein causes ribosome reduction and inhibition of protein synthesis in retinal pigment epithelial cells

Francesco Giorgianni *, Sarka Beranova-Giorgianni **

Department of Pharmaceutical Sciences, The University of Tennessee Health Science Center, Memphis, TN, USA

ARTICLE INFO

Keywords:
Retinal pigment epithelium
Oxidized LDL
Drusen
Proteome
Oxidative stress
Proteostasis

ABSTRACT

Retinal pigment epithelium (RPE) are specialized multifunctional cells indispensable for maintenance of vision. Dysfunction and death of the RPE cells is implicated in the genesis and progression of age-related macular degeneration (AMD). Oxidative stress and resulting cellular damage plays a critical mechanistic role in AMD pathogenesis. Oxidized low-density lipoprotein (oxLDL), derived from LDL in a pro-oxidative environment, is found adjacent to the RPE as part of drusen, extracellular deposits that are a characteristic clinical feature of AMD. OxLDL is cytotoxic and oxLDL-induced oxidative damage may contribute to functional impairment of the RPE. Therefore, knowledge of how the RPE respond to oxLDL exposure is important to understand the mechanisms underlying RPE dysfunction and death associated with AMD. The objective of this study was to characterize alterations in the RPE proteome triggered by exposure to non-cytotoxic levels of oxLDL. Protein identification and quantification were performed with a high -resolution LC-MS/MS-based proteomics workflow. In total, out of the *ca* 3000 RPE proteins quantified, oxLDL treatment caused expression changes of 303 proteins. As revealed by protein functional analysis, oxLDL uptake caused a multifaceted molecular response that involved numerous biological pathways. This response included up-regulation of anti-oxidative stress proteins whose expression is mediated by the transcription factor nuclear factor erythroid 2-related factor 2 (NRF2), confirming results of transcriptomics studies previously published by us and others. Significantly, and previously unreported, the oxLDL treatment induced down-regulation of ribosomal and translation initiation proteins, and up-regulation of proteins involved in autophagy, thus suggesting that a major cellular mechanism through which the RPE mitigate oxLDL-induced damage involves inhibition of protein synthesis and removal of misfolded proteins.

1. Introduction

The retinal pigment epithelium (RPE) are specialized cells in the macula that form a polarized monolayer located between photoreceptors and an extracellular matrix structure termed the Bruch membrane that separates the RPE from the choroidal vasculature [1]. The RPE are multifunctional cells primarily responsible for the maintenance and health of photoreceptors, and hence they are essential for vision. Age-dependent dysfunction and death of the RPE is linked to development of age-related macular degeneration (AMD), a leading cause of blindness in adults over 60 years of age in the US and other industrialized countries [2–4]. Oxidative stress and resultant molecular and cellular damage have been strongly implicated as contributors to the progressive dysfunction and loss of the RPE associated with AMD, in particular with the dry form of the disease [5,6]. The current lack of effective treatments for dry AMD underscores the significance of efforts aimed at understanding of mechanistic pathways underlying RPE dysfunction, which will in turn inform development of vision-saving therapies for AMD.

Oxidatively modified low-density lipoprotein (oxLDL) is an oxidative stress-inducing, cytotoxic agent formed from LDL in a pro-oxidant milieu through modification of its lipid and/or protein components [7]. OxLDL has been found in extracellular deposits (drusen) that accumulate in the sub-RPE space and are a prominent clinical feature of AMD [8,9]. Because of this association, the mechanisms of how the RPE respond when exposed to oxLDL are of high importance for understanding of the events involved in development and progression of AMD.

Unbiased systems biology approaches, including -omics strategies, are increasingly recognized as integral to research endeavors focusing on deciphering the molecular and cellular mechanisms that drive RPE

* Corresponding author.
** Corresponding author.
E-mail addresses: fgiorgia@uthsc.edu (F. Giorgianni), sberanova@uthsc.edu (S. Beranova-Giorgianni).

https://doi.org/10.1016/j.bbrep.2022.101345
Received 18 April 2022; Received in revised form 27 July 2022; Accepted 7 September 2022

dysfunction and AMD pathogenesis [10]. In our previous work we studied the global molecular response at the transcriptome level of RPE cells *in vitro* following short-term exposure to a non-cytotoxic dose of oxLDL [11]. We showed that upon oxLDL uptake, the RPE cells mount an extensive, multifaceted response evidenced by alterations affecting over 400 transcripts. From the functional standpoint, we found that these early transcriptome alterations elicited by oxLDL include activation of anti-antioxidant defense genes controlled by the transcription factors nuclear factor erythroid 2-related factor 2 (NRF2) and aryl hydrocarbon receptor (AhR), and down-regulation of elements of lipid metabolism, including genes involved in cholesterol biosynthesis. Furthermore, we discovered down-regulation of a set of genes related to circadian rhythm, which suggests that oxLDL may perturb circadian clock-dependent functions in the RPE [11].

In the study reported here we expand the global molecular profiling of the RPE response to oxLDL to interrogation of the RPE proteome. To determine protein expression changes induced by exposure of the cells to oxLDL, we used LC-MS/MS-based data-independent acquisition and label-free quantification to analyze the proteome in ARPE-19 cells following a 4 and 24 h treatment with oxLDL. We show that oxLDL modulates the expression of RPE proteins in multiple functional modules including proteins with anti-oxidative defense functions, glucose metabolism and lipid metabolism. Most significantly, we uncovered down-regulation of a large set of ribosomal assembly proteins and proteins involved in translation initiation, and up-regulation of autophagy proteins. This finding points to inhibition of protein synthesis and concomitant enhancement of intracellular degradation processes as major mechanisms through which the RPE respond to oxLDL-induced oxidative stress.

2. Materials and methods

2.1. Cell culture and Western Blot analysis

The experiments were performed with the immortalized human retinal pigment epithelial cell line ARPE-19. ARPE-19 cells were purchased from ATCC (Manassas, USA) and maintained in DMEM-F12 medium (ATCC, Manassas, USA) containing 2 mM L-glutamine supplemented with 10% fetal bovine serum (ATCC, Manassas, USA), 100 μg/mL of Primocin antibiotic (Invitrogen Carlsbad, USA) in a humidified atmosphere with 5% CO_2 at 37 °C. OxLDL (TBARS: 29–44 nmol MDA/mg) was obtained from Alfa Aesar (Tewksbury, USA). Cells (150,000) were seeded on 6 well plates and grown until confluence. Prior to oxLDL treatment, the ARPE-19 cells were maintained in serum-free medium for 24 h, and then treated with oxLDL (100 μg/mL) for 4 h and 24 h. In our previous studies we have determined that there is minimal cytotoxicity (<5% cell death) after 24 h exposure of ARPE-19 cells to oxLDL at this dose [11]. All experiments were performed in multiple biological replicates (n = 6). To validate increased expression of one of the top up-regulated proteins, heme oxygenase-1 (HO-1 or HMOX1), 60 μg of ARPE-19 cell protein extracts under different treatment conditions were separated on SDS-PAGE gels and transferred to a PVDF membrane. The membrane was incubated in blocking buffer (5% BSA in TBST) for 1 h at room temperature. After blocking, the membrane was incubated with a rabbit polyclonal anti-human HMOX1 antibody (ThermoFisher Scientific, PA5-27338, diluted 1:1000) and mouse polyclonal anti-human GAPDH antibody (Santa Cruz, sc-47724, diluted 1:1000) in blocking buffer overnight at 4 °C. After washing in TBST buffer, Alexa Fluor-conjugated secondary antibodies (ThermoFisher Scientific A-11008 and A-11029) were added at 1:10,000 dilution in 0.5% BSA/TBST. The membrane was incubated for 1 h, then washed with TBST buffer (6X). Reactive bands were visualized by fluorescence imaging on a Biotek Cytation 5 reader.

2.2. Protein processing and LC-MS/MS

Proteome analyses were performed as previously described [12]. Proteins extracted from control and oxLDL-treated cells (n = 6 per group) were digested with the iST sample preparation kit (PreOmics GmbH, Planegg/Martinsried, Germany) using the manufacturer's protocol with some modifications. Specifically, after digestion the peptide samples were dried in a speed vacuum centrifuge, and a custom solution (98% H_2O, 2% ACN, 0.1% TFA) was used instead of the manufacturer-supplied LC-Load solution to reconstitute the dried peptide samples. The peptide solutions were mixed in a 1:1 (v:v) ratio with an internal standard solution consisting of 25 fmol/μL yeast alcohol dehydrogenase 1 (ADH1, P00330) tryptic digest (Waters, Milford, USA). All peptide analyses were performed with a Synapt G2-*Si* quadrupole time-of-flight (QTOF) tandem mass spectrometer with ion mobility separation, IMS (Waters, Milford, USA), interfaced to an Acquity M-Class UPLC nano-LC system (Waters). The LC-MS/MS system was controlled via the MassLynx software suite (v. 4.1). To pre-concentrate the samples, the peptide solutions (2 μL) were injected on-line onto a Symmetry C18 trap column (100 Å, 5 μm, 180 μm × 20 mm; Waters). Peptides eluted from the trap were separated on a nano-flow UPLC C18 column (HSS T3, 1.8 μm, 75 μm × 250 mm; Waters) with a 180 min linear gradient of 2%–40% mobile phase B at a flow rate of 300 nL/min. Mobile phase B was ACN/0.1% formic acid and mobile phase A was H_2O/0.1% formic acid. The analytical column temperature was kept at 45 °C. The eluted peptides were ionized by nanoelectrospray, with source temperature set at 80 °C and capillary voltage of 2.8 kV. For lock-mass correction, [Glu1]-fibrinopeptide B standard was introduced concomitantly with the peptide analytes via infusion. The data were collected in a $HDMS^E$ (High Definition MS^E) data-independent acquisition mode [13], with the mass spectrometer acquisition parameters set into an $HDMS^E$ method created through MassLynx. The method included settings for the TOF to detect ions in the 50–2000 *m/z* range, and for the inclusion of IMS that preceded peptide precursor ion dissociation in the transfer cell. The TOF analyzer was operated in resolution mode (resolution >20,000 FWHM). Furthermore, the $HDMS^E$ method included optimized collision energy settings, with low collision energy set at 6 V and the high collision energy set to be precursor ion drift time-specific and ramped during acquisition from 17 V to 60 V [14,15].

2.3. Data analysis

The LC-MS/MS datasets were analyzed with the Progenesis QI for proteomics (v. 2.1, Nonlinear Dynamics) software platform. The software default peak-picking settings were used to process the raw data. Proteins were identified via the ProteinLynx Global Server (PLGS) search engine (v. 3.0.3, Waters) through searches of the Uniprot protein sequence database (human). The searches allowed up to 1 missed trypsin cleavage per peptide, static modification of cysteine (carbamidomethylation), and variable modification of methionine (oxidation). The peptide false discovery rate (FDR) was set to less than 4%. Label-free quantification was performed based on signal intensities by application of the "Hi-3″ method [16] using ADH1 as an internal calibrant for absolute quantification. The normalized protein abundance fold changes and related statistical significance among groups were calculated in Progenesis using the software default settings. Differentially expressed proteins were considered based on cutoff values of $|\text{fold change}| \geq 1.5$ and q value < 0.05.

For functional annotation, sets of differentially expressed proteins (up-regulated and down-regulated) were analyzed with the DAVID [17] and STRING [18] bioinformatics tools. Manual inspection of the differentially expressed protein datasets and searches of primary literature were also carried out to identify additional proteins/themes with mechanistic significance.

3. Results

To investigate the effects of oxLDL exposure on the proteome in RPE cells, we applied an LC-MS/MS-based quantitative proteomics workflow summarized in Fig. 1. In this workflow, separations of highly complex peptide mixtures produced by proteolytic digestion of whole RPE proteomes were carried out by ultra-high performance LC (UPLC) in the nanoflow regime. The data were acquired using the HDMS^E data-independent acquisition (DIA) method, which uses an additional dimension of analyte separation by inclusion of ion mobility (IMS) in the QTOF instrument platform. In conventional HDMS^E, the instrument is set to allow the collision energy to alternate between low and high values in order to generate full-mass range MS and fragment MS/MS spectra without precursor ion isolation. In our workflow, we used a modified HDMS^E approach that included application of IMS drift time-dependent ramping of collision energies as described by Distler *et* al. [14]. Peptide/protein quantification was performed with a label-free approach based on precursor ion signal intensities.

With our unbiased HDMS^E strategy, we identified and quantified a total of 2889 ARPE-19 proteins. Differential protein expression analysis revealed that exposure of ARPE-19 cells to non-cytotoxic levels of oxLDL for 24 h generated a reproducible and robust proteome response: in total, 303 proteins exhibited alterations induced by oxLDL (see Supplementary Table). Representative examples of peptide expression profiles are shown in Fig. 2 (A-B), together with validation by Western Blotting of one of the most up-regulated proteins (Fig. 2C). In the panel of differentially expressed proteins, 104 were up-regulated, and 199 were found to be down-regulated in response to oxLDL (Fig. 3A–B). The protein with the largest magnitude of change was heme oxygenase 1 (HO-1 or *HMOX1*), whose expression was up-regulated >19-fold after 24-h oxLDL treatment. This finding parallels our earlier ARPE-19 transcriptomic study, in which we observed up-regulation of *HMOX1* as by far the largest change following oxLDL exposure for 2 h and 4 h [11]. Of note, however, is the fact that, in contrast to the pronounced transcriptome alterations encompassing more than 400 genes after 4 h oxLDL treatment, early response at the proteome level assessed at the 4 h-exposure time point showed minimal alterations: within the probed set of ARPE-19 proteins, we found expression changes in only 4 proteins, including HO-1 (data not shown).

For functional annotation, the datasets of differentially expressed proteins up- or down-regulated upon oxLDL treatment were analyzed by the DAVID and STRING tools, together with additional manual inspection of the results. For the up-regulated proteins, this combined approach showed anti-oxidative stress response proteins and regulators of autophagy as the most prominent functional groups (Table 1). For the down-regulated proteins, major functional groups were represented by ribosome components and proteins involved in translational initiation (Table 1; Figs. 4 and 5). As revealed by the bioinformatics analyses of the down-regulated proteins, the most significantly enriched biological process was Translational Initiation (GO:0006413) encompassing 31 differentially expressed proteins (Figs. 4 and 5). It should also be noted that, in addition to the down-regulated proteins listed in Table 1, inspection of our raw data showed another large set of ribosomal components and translation initiation factor proteins (see Supplementary Table) whose expression was significantly down-regulated in oxLDL-treated cells even though the magnitude of the change was slightly below the 1.5-fold cutoff. Thus, the functional analyses results highlight an extensive negative impact of oxLDL on the cellular protein synthesis machinery.

4. Discussion

AMD is a multi-factorial, degenerative disorder of the central regions of the retina – the macula. By far, the most common form of the disease is dry AMD, which accounts for 85–90% of cases; at present there is no effective treatment for dry AMD. From the mechanistic standpoint, AMD is a complex disease, with an interplay of genetic and environmental risk factors contributing to disease development. Oxidative stress and resulting molecular alterations and cellular damage to the retina have been implicated as critical contributors in the mechanisms of AMD pathology. OxLDL is present *in vivo* in drusen, which are extracellular deposits that accumulate in areas adjacent to the RPE and represent a hallmark clinical sign of AMD. Even though AMD is usually a chronic disease with a multi-year development course, the acute effects caused by cytotoxic metabolites, such as oxLDL, are of relevance to understand the early mechanistic events that lead to RPE dysfunction and death in the context of AMD. Previous studies have shown the presence of oxidized lipoproteins in early AMD patient samples suggesting that oxLDL is a contributor in the early phase of the AMD phenotype [8].

OxLDL is generated through chemical modifications of LDL that generate oxidation-specific epitopes (OSE). It is the presence of oxidized moieties on oxLDL that triggers the targeting of this endogenous "modified self" biomolecule by the innate immune system through the action of scavenger receptors, which mediate the cellular uptake of oxLDL as part of protective clearance mechanisms essential for normal physiology [7,19]. We and others have shown that RPE internalize

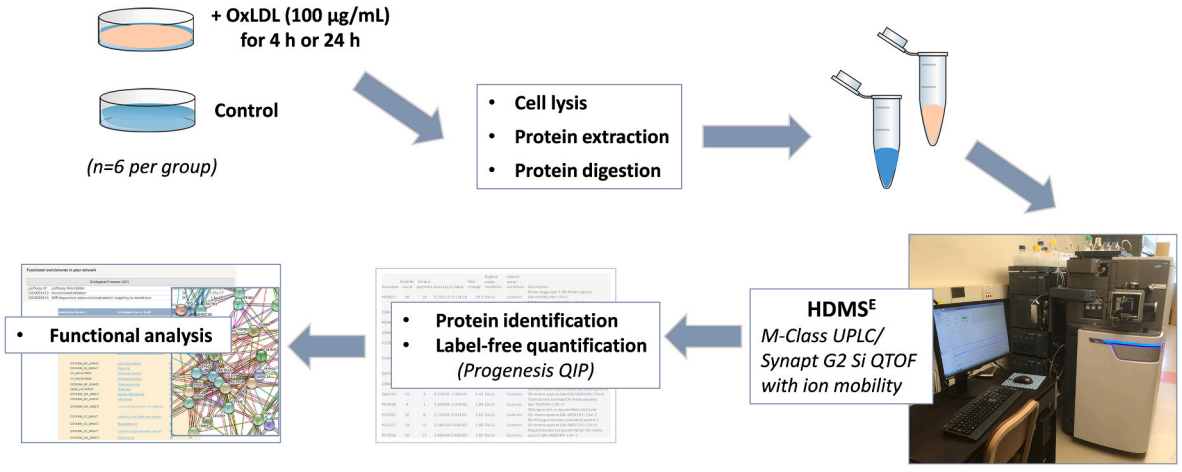

Fig. 1. Comparative proteomics analysis of ARPE-19 response to oxLDL. Replicates of whole protein extracts from ARPE-19 cells (oxLDL treated and control) were digested with trypsin. Desalted peptides were mixed with ADH1 (yeast alcohol dehydrogenase 1) as internal standard and analyzed by LC-MS/MS in the data-independent acquisition (DIA) mode. Label-free protein quantification was performed with Progenesis QIP. Data sets of differentially expressed proteins (|fold change| $\geq$ 1.5 and q value $<$ 0.05) were analyzed with DAVID and STRING for functional classification.

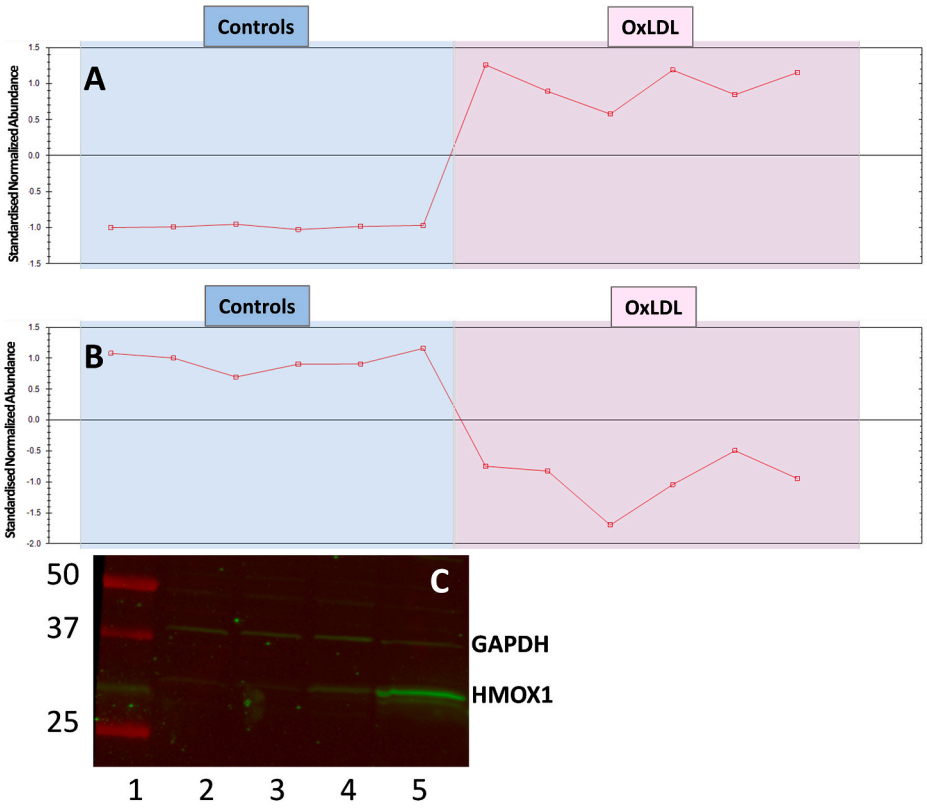

Fig. 2. Proteome changes in ARPE-19 following oxLDL treatment. (**a**) Peptide ion profile of heme oxygenase-1 (up-regulated); (**b**) peptide ion profile of 40S ribosomal protein S2 (down-regulated). (Each point in the peptide ion profile corresponds to a biological replicate); (**c**) WB analysis of ARPE-19 cell protein extracts: lane **1**-MW markers; **2**-untreated cells (4h); **3**-untreated cells (24h); **4**-oxLDL treated cells (4h); **5**-oxLDL treated cells (24h).

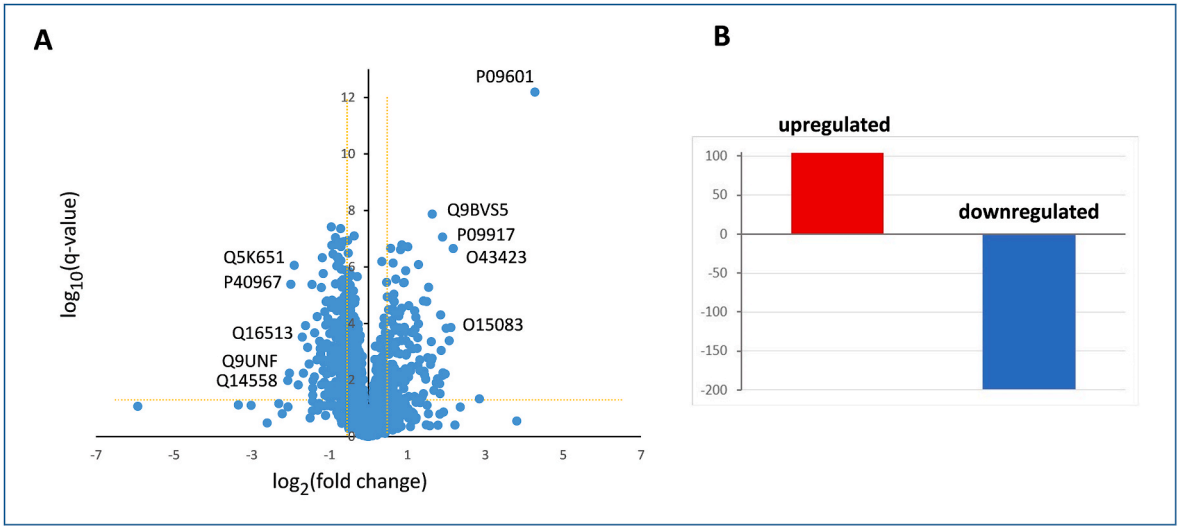

Fig. 3. Global proteome analysis of ARPE-19 following 24 h exposure to oxLDL. (**a**) Volcano plot of the mean expression fold-change versus significance following 24 h treatment with oxLDL. The horizontal dashed line represents the threshold limits for statistical significance (q = 0.05); the vertical dashed lines represent fold change threshold limits (≥± 1.5). Down-regulated proteins are on the left; up-regulated proteins are on the right. The top 5 most up- and down-regulated proteins are labeled with their respective Uniprot accession number. (**b**) Number of significantly up- and down-regulated proteins following exposure to oxLDL (fold change ≥1.5).

oxLDL primarily through the CD36 scavenger receptor [11,20–22]. Following oxLDL uptake, the RPE cells activate a multifaceted molecular response that encompasses alterations (up-regulation as well as down-regulation) in gene expression. As we reported recently, at the transcriptome level a 4 h exposure of RPE cells in culture to oxLDL resulted in expression changes of over 400 genes [11]. In contrast to the pronounced transcriptome alterations, at the proteome level (within the ca 3000 RPE proteins quantified with our bioanalytical workflow), after 4 h oxLDL exposure we only observed a few expression changes, the most relevant being the up-regulation of heme oxygenase 1 (HO-1), a molecular marker of cellular acute response to oxidative stress. However, extension of the oxLDL exposure time from 4 to 24 h induced a

Table 1
OxLDL-induced expression changes in selected proteins with high functional significance.

Uniprot accession number	Protein Name	Fold Change oxLDL/ ctrl
Anti-oxidant response		
P09601	Heme oxygenase 1	19.3
P15559	NAD(P)H dehydrogenase [quinone] 1	1.9
P48507	Glutamate-cysteine ligase regulatory subunit	1.9
Autophagy		
Q13501	Sequestosome-1	2.9
O94964	Protein SOGA1	1.8
P53365	Arfaptin-2	3.6
Glucose metabolism		
P29401	Transketolase	1.7
P37837	Transaldolase	1.8
Q01813	ATP-dependent 6-phosphofructokinase, platelet	−1.8
P17858	ATP-dependent 6-phosphofructokinase, liver	−2.3
P52790	Hexokinase-3	−1.5
P14618	Pyruvate kinase	−1.6
Lipid metabolism		
P37268	Squalene synthase	−1.9
Q16850	Lanosterol 14-alpha demethylase	−2.2
Translation initiation		
Q9BY44	Eukaryotic translation initiation factor 2A	−2.5
Q14152	Eukaryotic translation initiation factor 3	−1.8
P55010	Eukaryotic translation initiation factor 5	−1.7
P60842	Eukaryotic translation initiation factor 4A-I	−1.7
P05198	Eukaryotic translation initiation factor 2 subunit 1	−1.5
Q14240	Eukaryotic initiation factor 4A-II	−1.9
O00303	Eukaryotic translation initiation factor 3 subunit F	−1.5
O75822	Eukaryotic translation initiation factor 3 subunit J	−1.6
O15371	Eukaryotic translation initiation factor 3 subunit D	−1.5
Ribosome structure		
P61513	60S ribosomal protein L37a	−2.4
P62888	60S ribosomal protein L30	−2.3
P22090	40S ribosomal protein S4y isoform 1	−2.3
P46783	40S ribosomal protein S10	−1.9
P15880	40S ribosomal protein S2	−1.6
P46781	40S ribosomal protein S9	−1.6
P61247	40S ribosomal protein S3a	−1.6
P62081	40S ribosomal protein S7	−1.7
P62701	40S ribosomal protein S4_ X isoform	−1.6
P62249	40S ribosomal protein S16	−2.1
P62917	60S ribosomal protein L8	−1.5
P62244	40S ribosomal protein S15a	−1.6
P84098	60S ribosomal protein L19	−1.6
P62241	40S ribosomal protein S8	−1.6
P62910	60S ribosomal protein L32	−2.0
P42766	60S ribosomal protein L35	−2.2
P46777	60S ribosomal protein L5	−1.6
P62263	40S ribosomal protein S14	−1.5
P46779	60S ribosomal protein L28	−1.5
P62857	40S ribosomal protein S28	−1.6
P26373	60S ribosomal protein L13	−1.5
P46778	60S ribosomal protein L21	−2.0
Other - Protein Synthesis		
Q9Y4W2	Ribosomal biogenesis protein LAS1L	−1.9
Q9UHB9	Signal recognition particle subunit SRP68	−1.9
P26641	Elongation factor 1-gamma	−1.6
P13639	Elongation factor 2	−1.9

prominent proteome response encompassing ca 10% of the probed proteins. Functional analyses of the differentially expressed proteins revealed several themes within this multifaceted response. The most significant themes/findings at the proteome level were ribosome reduction and inhibition of protein synthesis, and up-regulation of autophagy. In addition, response of RPE to oxLDL as revealed by bioinformatics-aided functional analysis included alterations in anti-oxidative defense, glucose metabolism and lipid metabolism.

4.1. Antioxidant response

The RPE exist in a highly oxidative environment and are therefore highly susceptible to oxidative stress. Multiple sources contribute to this oxidative milieu: high metabolic activity, high partial pressure of oxygen, high amounts of polyunsaturated fatty acids (PUFAs), presence of retinal pigments and exposure to light [6]. In response to damaging effects of oxidative stress, the RPE have developed a complex set of anti-oxidant protective mechanisms. A central component of the RPE cytoprotective network is cytoprotection mediated through the transcription factor nuclear factor erythroid-2 related factor 2 (NRF2), which induces the expression of various detoxifying enzymes [6]. Ample evidence has established the importance of NRF2-controlled signaling in protective response of RPE to stress and injury [23]. Major contributors to the NRF2 mediated antioxidant cellular defense mechanism are the catalases (CAT) and superoxide dismutases (SOD) [24,25], the glutathione redox system [26], and the aldehyde dehydrogenases (ALDH). The ability to up-regulate the expression of cytoprotective genes, including the NRF2 system, is critical for restoring retinal homeostasis following oxidative stress challenge. Activation of NRF2 signaling has been shown to underlie, at least in part, the cytoprotective effects of diet-related compounds studied in the context of RPE, including the fatty acid DHA [27] and the dithiolethione D3T [28]. With aging and/or under influence of environmental factors such as cigarette smoking, the NRF2-controlled cytoprotective pathway may become impaired or insufficient to provide adequate anti-oxidant response. RPE in aging mice have been shown to exhibit a decreased ability to activate NRF2-mediated response, and this impairment resulted in accumulation of oxidatively modified lipids and proteins [29].

In our proteomics study, the HO-1 (*HMOX1*) up-regulation stands out, displaying the largest magnitude of increase in expression (>19 fold) in oxLDL-treated cells (24 h treatment) compared to controls. Furthermore, expression of the HO-1 protein was up-regulated after a 4 h oxLDL exposure (as the only protein within the proteome probed with our platform that was differentially expressed and up-regulated at this time point). HO-1 is a marker of cellular response to oxidized phospholipids (components of oxLDL) and its up-regulation through the cAMP responsive element-binding protein (CREB) is believed to represent a feedback mechanism to limit inflammation [30]. Many of the alterations in anti-oxidant defense identified at the proteome level were also observed as part of the early (4 h) transcriptome response to oxLDL study [11].

4.2. Glucose and lipid metabolism

Glucose catabolism involves conversion of glucose to glucose-6-phosphate (G6P) as the first step in glycolysis, which proceeds in 10 steps to produce pyruvate. Alternatively, G6P is routed to pentose phosphate pathway (PPP), which is responsible for production of NADPH and of ribose-5-phosphate for nucleotide synthesis. NADPH is a major anti-oxidant molecule that provides reducing power, and the PPP is upregulated under oxidative stress conditions to provide adequate amounts of NADPH [31]. In our study, differential profiling of the RPE proteome revealed oxLDL-induced expression changes in several enzymes catalyzing key reactions in glucose metabolism (Table 1). Specifically, we observed down-regulation of hexokinase-3 (HK3), phosphofructokinase (PFK, two isoforms), and of pyruvate kinase. These enzymes catalyze rate-limiting steps in glycolysis and constitute important regulatory points, in particular PFK which catalyzes the first committed reaction in glycolysis. Concomitantly with reduced expression of glycolytic enzymes critical for regulation of the pathway, our results showed an increased expression of transaldolase (TAL) and transketolase (TK), which catalyze reactions in the pentose phosphate pathway. Transketolase, whose expression is modulated by NRF2, has

Annotation Cluster 1	Enrichment Score: 20.23	Count	P_Value	Benjamini
GOTERM_BP_DIRECT	translational initiation	31	2.8E-30	2.6E-27
GOTERM_BP_DIRECT	SRP-dependent cotranslational protein targeting to membrane	23	4.2E-23	1.9E-20
GOTERM_BP_DIRECT	nuclear-transcribed mRNA catabolic process, nonsense-mediated decay	23	1.1E-20	3.3E-18
GOTERM_BP_DIRECT	viral transcription	22	6.1E-20	1.4E-17
GOTERM_BP_DIRECT	rRNA processing	24	3.6E-16	6.7E-14
GOTERM_BP_DIRECT	translation	25	1.5E-15	2.3E-13

Fig. 4. DAVID bioinformatics analysis of down-regulated proteins in oxLDL treated ARPE-19 cells. The top functional cluster includes proteins involved in translational initiation (GO:0006413).

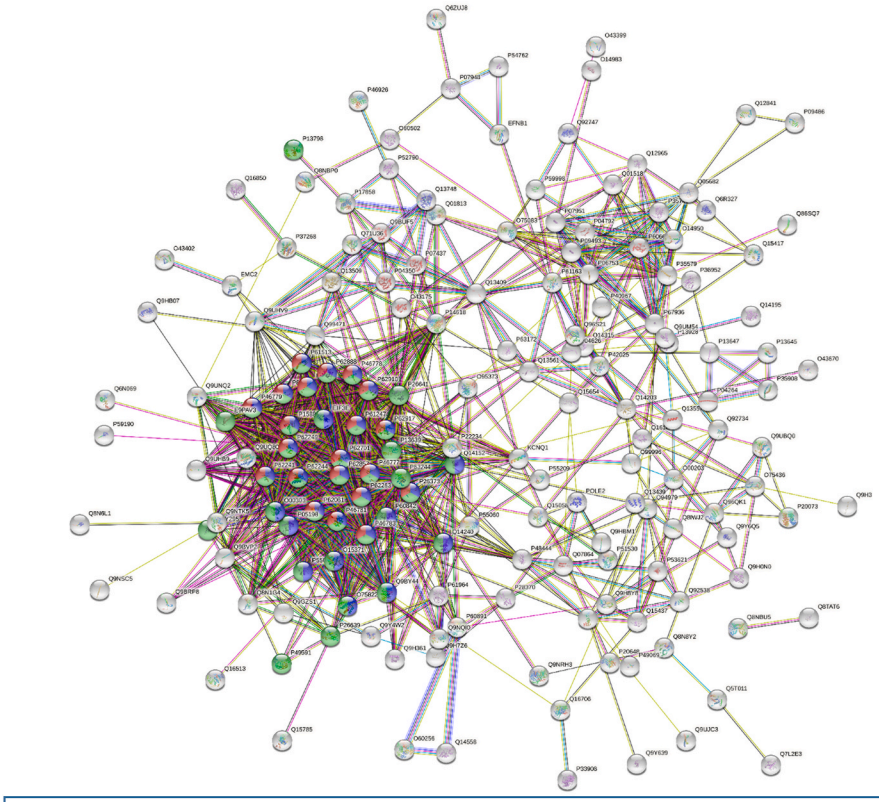

Biological Process (Gene Ontology)

GO-term	description	count in network	strength	false discovery rate
GO:0006413	translational initiation	31 of 141	1.33	1.10e-25
GO:0006412	translation	39 of 366	1.02	6.30e-23
GO:0006614	SRP-dependent cotranslational protein targeting to membra...	22 of 96	1.35	2.35e-18

KEGG Pathways

pathway	description	count in network	strength	false discovery rate
hsa03010	Ribosome	21 of 130	1.2	1.85e-15

Fig. 5. STRING bioinformatics analysis of the down-regulated proteins in oxLDL treated ARPE-19 cells. Nodes labeled with Uniprot accession numbers correspond to proteins, edges represent interactions. The highly interconnected region of the protein-protein interaction network corresponds to proteins (highlighted with colored circles) that are part of translation initiation pathways.

been shown to play a major role in counteracting oxidative stress through generation of NADPH in the PPP [32]. Overall, alterations in the expression of glycolytic and PPP enzymes observed in our proteomics analysis indicate oxLDL-induced effects on glucose metabolism and suggest that RPE respond to oxLDL exposure by enhancing metabolite flux to the pentose phosphate pathway for an increased production of NADPH to supply cellular NADPH-dependent antioxidant systems.

Aging-related depositions of lipids/lipoprotein particles occur in the Bruch membrane at the basolateral side of the RPE. Accumulation and subsequent oxidation of these retained lipids and lipoproteins are postulated to represent precursor events leading to formation of drusen, the hallmark lesions in AMD [9,33]. CD36-mediated uptake of oxidized lipoproteins by the RPE is suggested to function as a protective mechanism to clear sub-RPE deposits [20]. Internalization of oxidized LDL by the RPE exposes the cell to an increased load of cholesterol and oxidized cholesterol derivatives including 7-ketocholesterol [34]. In our proteomics study of the RPE response to oxLDL, the subset of proteins whose expression was down-regulated by oxLDL treatment includes two enzymes from the *de novo* cholesterol biosynthesis pathway: squalene synthase and lanosterol 14-alpha demethylase (CYP51A1). Squalene

synthase is involved in the formation of squalene, a key cholesterol precursor, and is an important regulatory point in cholesterol biosynthesis [35]. CYP51A1 catalyzes an early step in the lanosterol-to-cholesterol stage of cholesterol biosynthesis [36]. These results, obtained by examination of oxLDL effects at the proteome level are consistent with our earlier data from the RPE transcriptomics study that also revealed oxLDL-induced downregulation of enzymes from the cholesterol biosynthetic pathway [11]. Collectively, our findings point out that following uptake of oxLDL and intracellular release of its bioactive molecular components, the RPE response to the increased sterol levels includes attenuation of *de novo* cholesterol synthesis.

4.3. Ribosome reduction and protein synthesis inhibition

In our view, the most significant and novel finding of this study was the effect oxLDL exerted on protein homeostasis disruption. We found that more than a third of all known structural components of the ribosome where down-regulated together with proteins involved in ribosome biogenesis and numerous proteins involved in protein synthesis and proteins components of the signal-recognition particle (SRP) complex. These findings support a model for the toxicity of oxLDL that involves the down-regulation of pathways that promote protein synthesis, while at the same time proteins involved in degradation pathways are being up-regulated. Taken together, these data suggest a mechanism for oxLDL toxicity in the RPE that involves protein misfolding, with a decrease in protein synthesis and an increase of protein degradation pathways as a response to the proteotoxic agent, ultimately resulting in the reorganization of cellular proteostasis. OxLDL is generated by oxidative modifications of LDL through enzymatic and/or non-enzymatic routes, and encompasses a heterogeneous mixture of bioactive components including oxidized phospholipids, oxysterols, and oxidatively modified apoB 100. The presence of carbonyl groups (ketones and aldehydes), e.g. 4-hydroxynonenal and malondialdehyde, derived from lipid oxidation by reactive oxygen species [37–39] makes oxLDL capable to react with protein nucleophilic amino acids and modify them. These amino acid modifications ultimately cause protein misfolding, subsequent disruption of protein homeostasis and endoplasmic reticulum (ER) stress [40]. The cellular response to protein misfolding events involves the activation of the unfolded protein response (UPR) and autophagy pathways [41–43]. Both mechanisms balance protein synthesis with protein folding. Other studies in different cell models have shown that when excess of protein misfolding is detected the early cellular response includes reduction of protein synthesis. Similarly, the attenuation of protein synthesis through ribosome reduction and down-regulation of translation factors in our data indicate that the same mechanisms take place in the RPE 24 h following oxLDL treatment. Protein misfolding and dysregulated protein homeostasis have been implicated in numerous autoinflammatory pathologies [44] and age-related neurodegenerative diseases [45].

4.4. Autophagy

Autophagy is a highly conserved cellular degradation pathway for removal of damaged cellular components including misfolded proteins resulting from oxidative damage [46–48]. It is a lysosome-dependent process essential to the maintenance of cellular and tissue homeostasis [49]. The RPE, through autophagy-mediated cellular clearing processes metabolize spent photoreceptor outer segments (POS) and recycle their visual components, an essential function for the maintenance of a healthy retina. Due to their physiological role, the RPE have a very high metabolic rate and are located in an environment rich in oxygen and exposed to light, all factors that make them highly susceptible to oxidative damage [50]. Therefore, it is easy to recognize how crucial autophagy mechanisms are in the RPE and how their activation requires timely regulation at the transcriptional and post-transcriptional levels in response to changes in light and according to the organism's circadian rhythms [51]. It has been postulated that impairment of autophagy with age may contribute to the pathophysiological processes in AMD, including formation of extracellular drusen deposits [52]. Paralleling our transcriptomics findings [11], our proteomics investigation showed that exposure of the RPE to oxLDL results in an increased expression of sequestosome-1, a key regulator of autophagy and other autophagy-related proteins. This result provides further evidence that the cytoprotective response of the RPE to oxLDL-induced oxidative stress involves activation of autophagy, through activation of the KEAP1/NRF2 axis. Increased autophagy together with decreased protein synthesis suggest the activation of cytoprotective mechanisms aimed at reducing the intracellular accumulation of misfolded proteins, thus countering oxLDL-induced proteotoxicity.

5. Conclusions

We found that oxLDL exposure in RPE elicits a complex response that includes proteins with antioxidant properties, proteins involved in cellular clearance processes and a reduction of the cellular translational machinery; the latter response is an indication of an imbalance between *de novo* protein synthesis and proper protein folding. The cellular pathways involved in the attenuation of protein synthesis in the RPE remain to be elucidated, although examples are known in other cellular models that involve signal transduction mediated by PKR-like endoplasmic reticulum kinase (PERK) or the inositol-requiring enzyme 1 (IRE1) [53]. Guerra-Moreno et al. showed that arsenite-induced stress in yeast leads to increase protein degradation and reduced protein production through inhibition of the translation initiation factor eIF2-α, which is part of the PERK signal transduction pathway. They also reported reduction of ribosomal proteins that was independent of the eIF2-α inhibition pathway, suggesting a yet to be elucidated separate cellular mechanism [54]. Similarly, our data showed the inhibition of protein translation and a decrease of ribosomal proteins. While the exact cellular mechanisms involved in the RPE response to the proteotoxic agent remain to be elucidated, we believe that our study can be useful in the quest for a better understanding of AMD mechanisms and the identification of actionable targets/pathways such as the development of therapeutic agents that could restore the RPE proteostasis.

Author contributions

Conceptualization, methodology, validation, formal analysis, resources, data curation, visualization, project administration, funding acquisition: F.G. and S.B.G. Investigation, writing—original draft preparation, writing—review and editing: F.G., S.B.G. All authors have read and agreed to the published version of the manuscript.

Funding

This research was funded by the Retina Research Foundation, and the BrightFocus Foundation (grant number M2016068).

Declaration of competing interest

The authors declare no conflict of interest. The funders had no role in the design of the study; in the collection, analyses, or interpretation of data; in the writing of the manuscript, or in the decision to publish the results.

Acknowledgments

We thank Dr. Diwa Koirala for assistance with ARPE-19 cell culture and sample processing for proteome analyses.

Appendix A. Supplementary data

Supplementary data to this article can be found online at https://doi.org/10.1016/j.bbrep.2022.101345.

References

[1] O. Strauss, The retinal pigment epithelium in visual function, Physiol. Rev. 85 (3) (2005) 845–881.
[2] W.L. Wong, X. Su, X. Li, C.M.G. Cheung, R. Klein, C.-Y. Cheng, T.Y. Wong, Global prevalence of age-related macular degeneration and disease burden projection for 2020 and 2040: a systematic review and meta-analysis, Lancet Global Health 2 (2) (2014) e106–e116.
[3] https://www.nei.nih.gov/learn-about-eye-health/resources-for-health-educators/eye-health-data-and-statistics/age-related-macular-degeneration-amd-data-and-statistics.
[4] M. Fleckenstein, T.D.L. Keenan, R.H. Guymer, U. Chakravarthy, S. Schmitz-Valckenberg, C.C. Klaver, W.T. Wong, E.Y. Chew, Age-related macular degeneration, Nat. Rev. Dis. Prim. 7 (1) (2021) 31.
[5] C.B. Wright, J. Ambati, Dry age-related macular degeneration pharmacology, Handb. Exp. Pharmacol. 242 (2017) 321–336.
[6] S. Datta, M. Cano, K. Ebrahimi, L. Wang, J.T. Handa, The impact of oxidative stress and inflammation on RPE degeneration in non-neovascular AMD, Prog. Retin. Eye Res. 60 (2017) 201–218.
[7] I. Levitan, S. Volkov, P.V. Subbaiah, Oxidized LDL: diversity, patterns of recognition, and pathophysiology, Antioxidants Redox Signal. 13 (1) (2010) 39–75.
[8] Y. Yamada, J. Tian, Y. Yang, R.G. Cutler, T. Wu, R.S. Telljohann, M.P. Mattson, J. T. Handa, Oxidized low density lipoproteins induce a pathologic response by retinal pigmented epithelial cells, J. Neurochem. 105 (4) (2008) 1187–1197.
[9] J.T. Handa, M. Cano, L. Wang, S. Datta, T. Liu, Lipids, oxidized lipids, oxidation-specific epitopes, and Age-related Macular Degeneration, Biochim. Biophys. Acta 1862 (4) (2017) 430–440.
[10] J.T. Handa, C. Bowes Rickman, A.D. Dick, M.B. Gorin, J.W. Miller, C.A. Toth, M. Ueffing, M. Zarbin, L.A. Farrer, A systems biology approach towards understanding and treating non-neovascular age-related macular degeneration, Nat. Commun. 10 (1) (2019) 3347.
[11] D. Koirala, S. Beranova-Giorgianni, F. Giorgianni, Early transcriptomic response to OxLDL in human retinal pigment epithelial cells, Int. J. Mol. Sci. 21 (22) (2020) 8818.
[12] C. Parks, F. Giorgianni, B.C. Jones, S. Beranova-Giorgianni, B.M. Moore Ii, M. K. Mulligan, Comparison and functional genetic analysis of striatal protein expression among diverse inbred mouse strains, Front. Mol. Neurosci. 12 (2019) 128.
[13] J.C. Silva, R. Denny, C. Dorschel, M.V. Gorenstein, G.Z. Li, K. Richardson, D. Wall, S.J. Geromanos, Simultaneous qualitative and quantitative analysis of the Escherichia coli proteome: a sweet tale, Mol. Cell. Proteomics 5 (4) (2006) 589–607.
[14] U. Distler, J. Kuharev, P. Navarro, Y. Levin, H. Schild, S. Tenzer, Drift time-specific collision energies enable deep-coverage data-independent acquisition proteomics, Nat. Methods 11 (2) (2014) 167–170.
[15] D. Koirala, S. Beranova-Giorgianni, F. Giorgianni, Data-independent proteome analysis of ARPE-19 cells, Data Brief 20 (2018) 333–336.
[16] J.C. Silva, M.V. Gorenstein, G.-Z. Li, J.P. Vissers, S.J. Geromanos, Absolute quantification of proteins by LCMSE a virtue of parallel MS acquisition, Mol. Cell. Proteomics 5 (1) (2006) 144–156.
[17] B.T. Sherman, R.A. Lempicki, Systematic and integrative analysis of large gene lists using DAVID bioinformatics resources, Nat. Protoc. 4 (1) (2009) 44–57.
[18] D. Szklarczyk, A.L. Gable, D. Lyon, A. Junge, S. Wyder, J. Huerta-Cepas, M. Simonovic, N.T. Doncheva, J.H. Morris, P. Bork, STRING v11: protein–protein association networks with increased coverage, supporting functional discovery in genome-wide experimental datasets, Nucleic Acids Res. 47 (D1) (2019) D607–D613.
[19] C.J. Binder, N. Papac-Milicevic, J.L. Witztum, Innate sensing of oxidation-specific epitopes in health and disease, Nat. Rev. Immunol. 16 (8) (2016) 485–497.
[20] E. Picard, M. Houssier, K. Bujold, P. Sapieha, W. Lubell, A. Dorfman, J. Racine, P. Hardy, M. Febbraio, P. Lachapelle, H. Ong, F. Sennlaub, S. Chemtob, CD36 plays an important role in the clearance of oxLDL and associated age-dependent sub-retinal deposits, Aging (Albany NY) 2 (12) (2010) 981–989.
[21] G. Gnanaguru, A.R. Choi, D. Amarnani, P.A. D'Amore, Oxidized lipoprotein uptake through the CD36 receptor activates the NLRP3 inflammasome in human retinal pigment epithelial cells, Invest. Ophthalmol. Vis. Sci. 57 (11) (2016) 4704–4712.
[22] N. Gordiyenko, M. Campos, J.W. Lee, R.N. Fariss, J. Sztein, I.R. Rodriguez, RPE cells internalize low-density lipoprotein (LDL) and oxidized LDL (oxLDL) in large quantities in vitro and in vivo, Invest. Ophthalmol. Vis. Sci. 45 (8) (2004) 2822–2829.
[23] S. Felszeghy, J. Viiri, J.J. Paterno, J.M. Hyttinen, A. Koskela, M. Chen, H. Leinonen, H. Tanila, N. Kivinen, A. Koistinen, Loss of NRF-2 and PGC-1α genes leads to retinal pigment epithelium damage resembling dry age-related macular degeneration, Redox Biol. 20 (2019) 1–12.
[24] I. Venza, M. Visalli, M. Cucinotta, D. Teti, M. Venza, Association between oxidative stress and macromolecular damage in elderly patients with age-related macular degeneration, Aging Clin. Exp. Res. 24 (1) (2012) 21–27.
[25] I. Venza, M. Visalli, R. Oteri, D. Teti, M. Venza, Combined effects of cigarette smoking and alcohol consumption on antioxidant/oxidant balance in age-related macular degeneration, Aging Clin. Exp. Res. 24 (5) (2012) 530–536.
[26] M. Güven, E. Görgün, M. Ünal, M. Yenerel, B. Batar, B. Küçümen, U.A. Dinç, G. Güven, T. Ulus, A. Yüksel, Glutathione S-transferase M1, GSTT1 and GSTP1 genetic polymorphisms and the risk of age-related macular degeneration, Ophthalmic Res. 46 (1) (2011) 31–37.
[27] I. Johansson, V.T. Monsen, K. Pettersen, J. Mildenberger, K. Misund, K. Kaarniranta, S. Schonberg, G. Bjorkoy, The marine n-3 PUFA DHA evokes cytoprotection against oxidative stress and protein misfolding by inducing autophagy and NFE2L2 in human retinal pigment epithelial cells, Autophagy 11 (9) (2015) 1636–1651.
[28] K.R. Li, S.Q. Yang, Y.Q. Gong, H. Yang, X.M. Li, Y.X. Zhao, J. Yao, Q. Jiang, C. Cao, 3H-1,2-dithiole-3-thione protects retinal pigment epithelium cells against Ultra-violet radiation via activation of Akt-mTORC1-dependent Nrf2-HO-1 signaling, Sci. Rep. 6 (2016), 25525.
[29] M.M. Sachdeva, M. Cano, J.T. Handa, Nrf2 signaling is impaired in the aging RPE given an oxidative insult, Exp. Eye Res. 119 (2014) 111–114.
[30] G. Krönke, V.N. Bochkov, J. Huber, F. Gruber, S. Blüml, A. Fürnkranz, A. Kadl, B. R. Binder, N. Leitinger, Oxidized phospholipids induce expression of human heme oxygenase-1 involving activation of cAMP-responsive element-binding protein, J. Biol. Chem. 278 (51) (2003) 51006–51014.
[31] C. Riganti, E. Gazzano, M. Polimeni, E. Aldieri, D. Ghigo, The pentose phosphate pathway: an antioxidant defense and a crossroad in tumor cell fate, Free Radic. Biol. Med. 53 (3) (2012) 421–436.
[32] I.M. Xu, R.K. Lai, S.H. Lin, A.P. Tse, D.K. Chiu, H.Y. Koh, C.T. Law, C.M. Wong, Z. Cai, C.C. Wong, I.O. Ng, Transketolase counteracts oxidative stress to drive cancer development, Proc. Natl. Acad. Sci. U. S. A. 113 (6) (2016) E725–E734.
[33] T. Yasukawa, P. Wiedemann, S. Hoffmann, J. Kacza, W. Eichler, Y.S. Wang, A. Nishiwaki, J. Seeger, Y. Ogura, Glycoxidized particles mimic lipofuscin accumulation in aging eyes: a new age-related macular degeneration model in rabbits, Graefes Arch. Clin. Exp. Ophthalmol. 245 (10) (2007) 1475–1485.
[34] I.R. Rodriguez, S. Alam, J.W. Lee, Cytotoxicity of oxidized low-density lipoprotein in cultured RPE cells is dependent on the formation of 7-ketocholesterol, Invest. Ophthalmol. Vis. Sci. 45 (8) (2004) 2830–2837.
[35] J. Pandit, D.E. Danley, G.K. Schulte, S. Mazzalupo, T.A. Pauly, C.M. Hayward, E. S. Hamanaka, J.F. Thompson, H.J. Harwood Jr., Crystal structure of human squalene synthase. A key enzyme in cholesterol biosynthesis, J. Biol. Chem. 275 (39) (2000) 30610–30617.
[36] G.I. Lepesheva, M.R. Waterman, Sterol 14alpha-demethylase cytochrome P450 (CYP51), a P450 in all biological kingdoms, Biochim. Biophys. Acta 1770 (3) (2007) 467–477.
[37] A. Amici, R.L. Levine, L. Tsai, E.R. Stadtman, Conversion of amino acid residues in proteins and amino acid homopolymers to carbonyl derivatives by metal-catalyzed oxidation reactions, J. Biol. Chem. 264 (6) (1989) 3341–3346.
[38] A.G. Madian, A.D. Myracle, N. Diaz-Maldonado, N.S. Rochelle, E.M. Janle, F. E. Regnier, Differential carbonylation of proteins as a function of in vivo oxidative stress, J. Proteome Res. 10 (9) (2011) 3959–3972.
[39] G. Vistoli, D. De Maddis, A. Cipak, N. Zarkovic, M. Carini, G. Aldini, Advanced glycoxidation and lipoxidation end products (AGEs and ALEs): an overview of their mechanisms of formation, Free Radic. Res. 47 (Suppl 1) (2013) 3–27.
[40] D.S. Varghese, B.R. Ali, Pathological crosstalk between oxidized LDL and ER stress in human diseases: a comprehensive review, Front. Cell Dev. Biol. 9 (2021) 1276.
[41] J. Grootjans, A. Kaser, R.J. Kaufman, R.S. Blumberg, The unfolded protein response in immunity and inflammation, Nat. Rev. Immunol. 16 (8) (2016) 469–484.
[42] M. Kitamura, Endoplasmic reticulum stress and unfolded protein response in renal pathophysiology: Janus faces, Am. J. Physiol. Ren. Physiol. 295 (2) (2008) F323–F334.
[43] S. Matus, F. Lisbona, M. Torres, C. Leon, P. Thielen, C. Hetz, The stress rheostat: an interplay between the unfolded protein response (UPR) and autophagy in neurodegeneration, Curr. Mol. Med. 8 (3) (2008) 157–172.
[44] A.F. Agyemang, S.R. Harrison, R.M. Siegel, M.F. McDermott, Protein misfolding and dysregulated protein homeostasis in autoinflammatory diseases and beyond, Semin. Immunopathol. 37 (4) (2015) 335–347.
[45] J. Labbadia, R.I. Morimoto, The biology of proteostasis in aging and disease, Annu. Rev. Biochem. 84 (2015) 435–464.
[46] J. Zhang, Y. Bai, L. Huang, Y. Qi, Q. Zhang, S. Li, Y. Wu, X. Li, Protective effect of autophagy on human retinal pigment epithelial cells against lipofuscin fluorophore A2E: implications for age-related macular degeneration, Cell Death Dis. 6 (2015), e1972.
[47] N. Chondrogianni, I. Petropoulos, S. Grimm, K. Georgila, B. Catalgol, B. Friguet, T. Grune, E.S. Gonos, Protein damage, repair and proteolysis, Mol. Aspect. Med. 35 (2014) 1–71.
[48] S.K. Mitter, H.V. Rao, X. Qi, J. Cai, A. Sugrue, W.A. Dunn Jr., M.B. Grant, M. E. Boulton, Autophagy in the retina: a potential role in age-related macular degeneration, Adv. Exp. Med. Biol. 723 (2012) 83–90.
[49] D.C. Rubinsztein, G. Marino, G. Kroemer, Autophagy and aging, Cell 146 (5) (2011) 682–695.
[50] K. Kaarniranta, A. Koskela, S. Felszeghy, N. Kivinen, A. Salminen, A. Kauppinen, Fatty acids and oxidized lipoproteins contribute to autophagy and innate immunity responses upon the degeneration of retinal pigment epithelium and development of age-related macular degeneration, Biochimie 159 (2019) 49–54.
[51] J. Yao, L. Jia, S.J. Shelby, A.M. Ganios, K. Feathers, D.A. Thompson, D.N. Zacks, Circadian and noncircadian modulation of autophagy in photoreceptors and retinal pigment epithelium, Invest. Ophthalmol. Vis. Sci. 55 (5) (2014) 3237–3246.

[52] K. Kaarniranta, P. Tokarz, A. Koskela, J. Paterno, J. Blasiak, Autophagy regulates death of retinal pigment epithelium cells in age-related macular degeneration, Cell Biol. Toxicol. 33 (2) (2017) 113–128.
[53] P. Walter, D. Ron, The unfolded protein response: from stress pathway to homeostatic regulation, Science 334 (6059) (2011) 1081–1086.
[54] A. Guerra-Moreno, M. Isasa, M.K. Bhanu, D.P. Waterman, V.V. Eapen, S.P. Gygi, J. Hanna, Proteomic analysis identifies ribosome reduction as an effective proteotoxic stress response, J. Biol. Chem. 290 (50) (2015) 29695–29706.